Designing of carbon fiber-reinforced polymer (CFRP) composites for a second-life in the aeronautic industry: strategies towards a more sustainable future

Carolina Borges[1], A. Chícharo[1], A. Araújo[1,2], J. Silva[1] and R. M. Santos[1,2]*

[1]Materials and Composite Structures Unit, Institute of Science and Innovation in Mechanical and Industrial Engineering (INEGI), Porto, Portugal, [2]LAETA—Associated Laboratory of Energy, Transports and Aeronautics, Porto, Portugal

Over the last few years, the use of carbon fiber-reinforced polymer composites (CFRP) in the aeronautic sector has significantly increased, given these materials' outstanding properties. Consequently, the accumulation of composite residues is becoming an environmental hurdle. Therefore, in a world where sustainability and circularity remain on the lead, the replacement of thermosets by thermoplastics as polymeric matrices emerges as a promising technique, given the recyclability of these materials. Following this perspective, in this work, carbon fiber-reinforced polymer (CFRP) composite "residues" were incorporated into a poly(etheretherketone) (PEEK) matrix, as a strategy towards a more sustainable future, aiming at developing novel compounds for the aeronautic industry. The influence of two different fiber sizes (<600 and 600−1000 µm) on the neat PEEK properties was assessed through formulations developed using a co-rotating twin screw-extruder, under optimized processing conditions. Furthermore, the potential thermo-oxidative degradation, and the recycling feasibility of the neat PEEK and its compounds, were evaluated by submitting the materials to several thermo-mechanical cycles. The results showed that PEEK compounds were successfully prepared, and presented a good fiber distribution and absence of fiber agglomerates. A positive impact on the mechanical performance of PEEK was found by the incorporation of 3.3 wt.% of short carbon fibers (sCF) with larger sizes (600−1000 µm). The reprocessing of neat PEEK and its compounds for 15 consecutive cycles demonstrated their remarkable thermo-mechanical stability, without any sign of degradation or irreversible loss of properties. The fiber length and fiber length distribution of reprocessed compounds showed that major variations occurred after the first extrusion cycle, especially for larger sizes.

KEYWORDS

composites, recycling, compounding, extrusion, circular economy

1 Introduction

Carbon fiber-reinforced polymer (CFRP) composites scored tremendous scope of application in several flourishing sectors, including aerospace, construction, automotive, and wind energy fields, owing to their outstanding in-plane mechanical properties combined with lower density (Yao et al., 2018; Li and Englund, 2017; Pimenta and Pinho, 2011). Moreover, the soaring demand

for CFRPs in these sectors stems from their ease of integration, multifunctionality, and freedom in design of complex geometries and structures (Vo Dong et al., 2018; Zhang et al., 2020a; Giorgini et al., 2020; Butenegro et al., 2021). With all its major employers holding a substantial share in the modern economy, in 2020 the aviation, aerospace, and defense segments remained in the lead, in terms of share growth in the global CFRP composites market, reaching up to $7.0 billion, and by 2030 it is foreseen to reach $15.4 billion (Nikhil and ChidanandEswara, 2022).

Regarding the aerospace industry, CFRP composites are mainly applied to interiors, engine blades, propellers/rotors, brackets, single-aisle and wide-body wings, and nowadays, these materials represent up to 40% of modern aircraft. An example is the Boeing 787 Dreamliner passenger plane, which is composed by approximately 50% of composite materials by weight in the main body, parts of the tail, wings, and fuselage, becoming the most fuel-efficient aircraft (Fortune Business Insights, 2023). Furthermore, structural components based on CFRP composites can lead not only to a significant weight reduction but also to an important decrease of carbon dioxide (CO_2) emissions by up to 20%, during operations. In fact, CO_2 is the primarily emitted greenhouse gas, and its reduction can lead to global warming and climate change mitigation (Al-Lami et al., 2018).

Supported by sustainable and energy-efficiency trends, the global growth of CFRPs usage has unavoidably brought about a concomitant increase in production wastes and end-of-life (EoL) components (e.g., from decommissioned aircraft) (Pulkkinen, 2022), (Meng et al., 2020). According to the International Air Transport Association (IATA), nearly around 16,000 commercial passenger and cargo planes have been retired worldwide in the past 35 years and every year up to 700 jets are getting closer to the end of their operational lives. Moreover, the UK-based aerospace strategy consultancy, NAVEO, projected that at least 11,000 passenger and cargo planes will be officially retired from service over the next 10 years (Petrauskaite, 2022), (IATA, 2022). For aircrafts containing CFRPs in their composition, it is estimated that by 2025, 8,500 will be discarded, which will roughly translate to more than 154,000 tons of carbon fibers (CFs) (Meng et al., 2020), (Carberry, 2006), (Alves et al., 2018). Under this scenario, and towards a more circular economy, aircraft decommissioning is becoming an uppermost concern, involving a multidisciplinary process that encompasses environmental, operational, safety, legal, and economic aspects (Elsayed and Roetger, 2022).

Nevertheless, associated to traditional CFRPs design, manufacturing, and application, great challenges arise: the difficulty in reusing and recycling these materials, as well as the lack of sustainable and profitable recycling methodologies. These drawbacks are mainly promoted by i) their complex composition at different scales (fibers, matrix, and fillers), ii) the crosslinked nature of thermoset matrices, not allowing them to be remolded, reshaped, or recycled, and iii) their combination with other materials (metal fixings, honeycombs, among others). In the recent past, the main disposal routes of EoL composite structures include graveyards, landfills, or incineration, which are at the bottom of the waste management hierarchy. Therefore, turning CFRP "wastes" into a valuable material resource and closing the loop in the CFRP life cycle becomes primordial (Li and Englund, 2017), (Pimenta and Pinho, 2011).

Regardless of the different recycling methodologies, and their inherent advantages or disadvantages, mechanical recycling is the most technologically mature CFRP recycling method, which generally consists of reducing the material size to be further incorporated as a reinforcement or filler into new matrices (e.g., polymers, cement, among others) (Butenegro et al., 2021), (Giorgini et al., 2020), (Meng et al., 2020), (Oliveux et al., 2015; Vincent et al., 2019; Gao et al., 2022). Beyond mechanical methods, chemical recycling is a promising and complementary alternative to overcome the challenges inherent to traditional CFRP composites, allowing the recovery of valuable CFs through the depolymerization of the network structure by the cleavage of specific bonds presented in cured thermosets. However, chemical recycling demands harsh conditions, including high temperatures and pressures, and involves the presence of solvents and the production of various by-products (Liu et al., 2022), (Zhang et al., 2020b).

In an ever-evolving world, the development of more sustainable materials with improved properties and functionalities, ensuring they fit into the category of circular economy materials, is also an essential aspect to meet industrial demands, and prevent environmental and safety risks. In this sense, the replacement of thermosets by thermoplastics seems to be a promising route, and so far, significant efforts have been devoted to developing high-performance and -temperature polymers from the poly (aryletherketone) (PAEK) family, with special focus on poly (etheretherketone) (PEEK), for highly demanding applications (Lu et al., 2019a; Sudhin et al., 2020; Alshammari et al., 2021).

PEEK is a semi-crystalline thermoplastic with good chemical resistance, flame retardancy, low moisture absorption, and recyclability. This material is also known by its remarkable thermal stability provided by the presence of ether linkages in the molecular chain, which also imparts the possibility of being processable via cost-efficient and faster processes, such as injection molding and extrusion. However, its unusual mechanical performance is strongly dependent on the degree of crystallinity and crystalline morphology, which are influenced by the thermal history and processing conditions applied to the material. Therefore, the further structural reinforcement of PEEK with recovered CFRP "residues" or recycled CFs opens a new horizon for designing composite materials with enhanced mechanical wear and impact resistance, which are properties mainly required for the aeronautic industrial field (Lu et al., 2019b; Pedoto et al., 2022; Lu et al., 2023).

An overview of the literature reveals that few studies have been conducted aiming at establishing correlations between the orientation state of fibers, fiber length, fiber/matrix interface, and matrix crystallinity with the overall mechanical performance and microstructure of the recycled PEEK compounds (Zhang et al., 2012; Kumar, et al, 2008; Hirayama et al., 2017; Nakashima et al., 2017; Li et al., 2018; Subhedar et al., 2020). Thus, in the present work, carbon fiber-reinforced thermoplastic "residues" (rCFRT), resulting from the design, production and optimization of an aeronautic demo case (bracket), were milled and reused for the development of novel compounds. Two fiber sizes of rCFRT were selected and incorporated into a neat PEEK matrix to study their influence on the mechanical performance, thermal transitions and crystallinity degree, and rheological properties of the matrix. In addition, the developed compounds were further submitted to continuous thermo-mechanical cycles to investigate their potential thermo-oxidative degradation and recycling feasibility. The fiber length size and distribution, after several thermomechanical cycles, were also evaluated. The final objective of this work will be to reach the most suitable formulation, with tailored properties, which will be applied to develop another demo case by injection molding: an airplane bracket.

Afterward, three demo cases will be combined to produce a window frame by *in situ* welding.

2 Experimental part

2.1 Materials

The two materials used in this work were: 1) PEEK 150G pellets supplied by Victrex® (Lanchashire, United Kingdom), and 2) a low melt poly (aryletherketone), LMPAEK, unidirectional carbon fiber prepreg tapes. PEEK has a Newtonian plateau melt viscosity of 130 Pa.s at 400°C, a density of 1.30 g/cm³ at 25°C, and was used as a polymeric matrix. The "residues" from the carbon fiber reinforced low melt thermoplastics (rCFRT) were milled in a granulator (Rapid Granulator 200-24K®) with a 4 mm grid. All materials were previously dried overnight in an oven at 120°C and then subjected to a granulometric analysis by sieving in a sieve shaker (AS200 Analytical, Retsch®). The results are depicted in Figure 1.

The largest amount of rCFRT is in the range between 600 and 1,000 μm. Therefore, in this work, the incorporation of two different particle sizes was considered i) < 600 and ii) 600–1,000 μm.

2.2 Development of novel recycled compounds based on rCFRT

The development of novel recycled compounds, based on two different rCFRT sizes, was conducted in an intermeshing co-rotating twin-screw extruder (Coperion GmbH ZSK 26 Mc) with L/D = 40, with screws rotating at 200 rpm, to ensure adequate hydrodynamic shear stresses and residence times for the dispersion of rCFRT. Downstream accessories were coupled to the extruder, including a water-cooling bath, counter-current air dryer, and rotating knife. The loading of rCFRT was set at 5 wt% (selected based on a preliminary study conducted through i) rCFRT incorporations up to 10 wt%, without significant mechanical reinforcement of the compound between 5 and 10 wt%, and an assumption considering ii) the possible scarcity of the available "residues," with 5 wt% being a reasonable loading that guarantees the existence of enough rCFRT to be incorporated). In addition, it is relevant to state that in the bulk, this percentage only represents 3.3 wt% of CFs, since the LMPAEK tapes are constituted by 66% of CF weight fraction and 34% of PAEK. The screw configuration contains three mixing zones consisting of kneading blocks with different staggering angles, with the aim of melting the polymer and inducing dispersive mixing, separated by conveying sections. Extruded filaments with a 3 mm diameter were slowly cooled to ensure appropriate material recrystallization, and were then pelletized. The extrusion parameters were adjusted for each developed compound to ensure processing stability, and the data are presented in Table 1.

Table 1 shows the effect of reinforced PEEK with 5 wt% of rCFRT on the extrusion processing parameters, including pressure drop, and melt temperature. Since the melt temperature of compounds is similar to neat PEEK, significant increments in the melt viscosity or viscous dissipation with an incorporation of 5 wt% of rCFRT are not expected. However, it is important to note that even when extrusion processing conditions were adjusted (e.g., temperature profile), the incorporation of rCFRT had an adverse effect on processability, inducing a significant increase in the melt pressure, from 22–23 to 30–31 bar.

2.3 Samples preparation by injection and compression molding

Neat PEEK and its compounds containing 5 wt% of rCFRT were prepared by injection or compression molding, depending on the characterization technique requirements. For tensile tests, the materials were previously dried and injected in the form of type 1A specimens, according to ISO 527-2 standard, using an Engle ES 200/45 HL-V machine. Based on the safety data sheet provided by Victrex®,
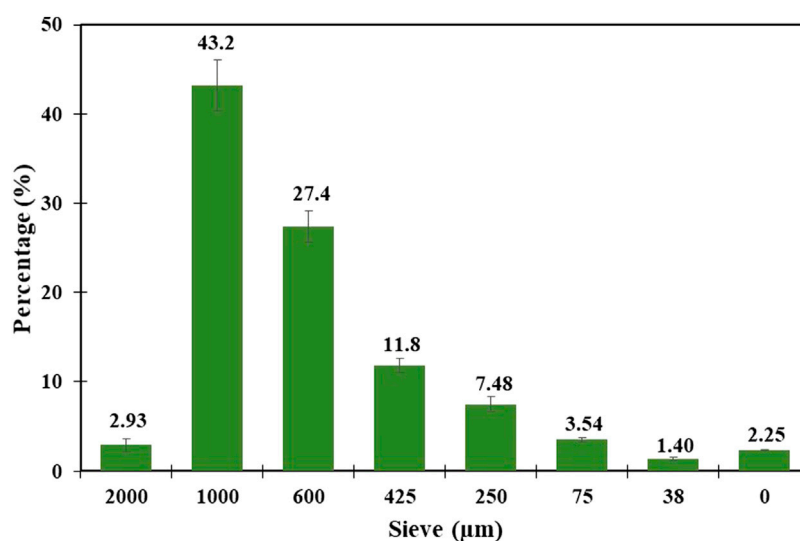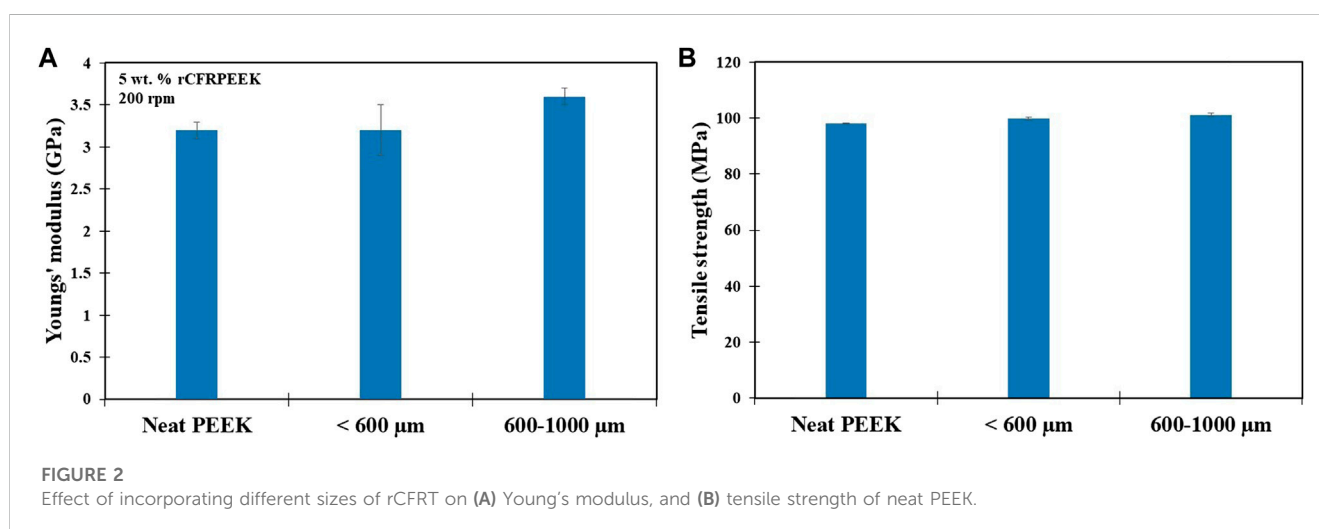

FIGURE 1
Granulometric analysis of the rCFRT.

TABLE 1 Adjusted extrusion processing conditions for each compound.

Formulation	Temperature profile (°C)	Pressure (bar)	Melt temperature (°C)
Neat PEEK	365-365-370-370-365-365-365-365-365-370	22–23	365–366
< 600 μm	360-365-365-370-370-370-375-375-375-375	28–30	364–365
600–1,000 μm	360-365-365-370-370-370-375-375-375-375	30–31	365–366

TABLE 2 Injection molding conditions.

Formulation	Injection temperatures (°C)	Mold temperature (°C)	Screw rotation (L/min)	Counter pressure (bar)	Injection pressure (bar)
Neat PEEK	350–380	210	100	50	857
< 600 μm	340–380	210	100	100	781
600–1,000 μm	340–380	210	100	100	781

FIGURE 2
Effect of incorporating different sizes of rCFRT on **(A)** Young's modulus, and **(B)** tensile strength of neat PEEK.

the recommended tool temperatures to obtain crystalline components with PEEK stand between 170 and 200°C. The barrel temperature range must stand between 350 and 380°C. PEEK compounds required increased barrel temperatures (maximum 20°C). Table 2 displays the injection molding conditions applied for injected bars.

For the rheological characterization, disks with 25 mm diameter and 1 mm thick were also prepared by compression molding in a hot plate press SATIM TYPE PML 1, at 390°C for 30 min.

2.4 Compounds' characterization

2.4.1 Stress-strain behavior

The influence of different rCFRT sizes on the quasi-static mechanical behavior of neat PEEK was evaluated using an INSTRON 4208® universal instrument (INSTRON, Massachusetts, United States), with a load cell of 5 kN and a constant crosshead speed of 2 mm/min until 4 mm displacement, followed by 10 mm/min up to mechanical failure. The data analysis
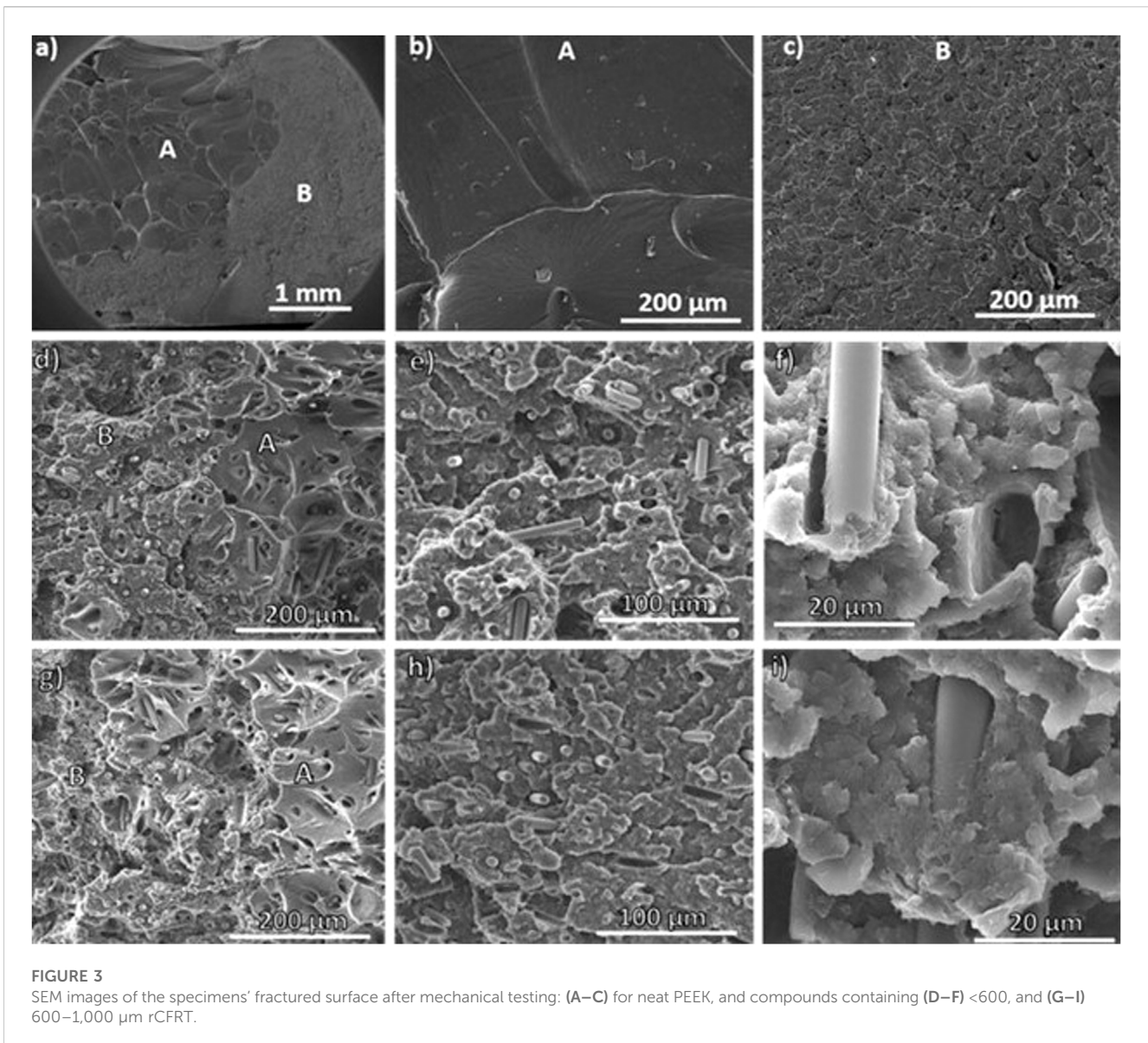
was assessed by means of ISO-527 standard tensile tests to determine compounds' ultimate tensile strength and Young's modulus.

2.4.2 Fractured surface observation by scanning electron microscopy (SEM)

The fractured surface of the tensile test specimens was observed using a High resolution (Schottky) Environmental Scanning Electron Microscope (FEI Quanta 400 FEG ESEM/EDAX Genesis X4M). Before the analysis, the samples were coated with a gold/palladium (Au/Pd) thin film for 120 s, and with a 15 mA current (SPI Module Sputter Coater).

2.4.3 Crystallization degree evaluation by differential scanning calorimetry (DSC)

The comparison between the crystallization degree and thermal transitions of neat PEEK and its compounds was assessed by DSC (TA Instruments Q20 model®, New Castle DE, United States). Samples were heated from 100.0 to 380.0°C at a heating rate of 30.0°C/min, under a nitrogen atmosphere. Afterwards, the samples were cooled up to

FIGURE 3
SEM images of the specimens' fractured surface after mechanical testing: **(A–C)** for neat PEEK, and compounds containing **(D–F)** <600, and **(G–I)** 600–1,000 μm rCFRT.

100.0°C and heated again from 100.0 to 380.0°C at 30.0°C/min. The reported results are the average of three tested samples, and the crystallinity degree of compounds was calculated as follows: $X_C = \frac{\Delta H_m}{\alpha \times \Delta H_{100\%}} \times 100$ (Lu et al., 2019c).

Where, Xc is the samples crystallinity degree, ΔH_m is the melting enthalpy during the second heating, $\Delta H_{100\%}$ = 130 J/g (Lu et al., 2019c) is the melting enthalpy for fully crystalized PEEK, and α is the mass fraction of PEEK in the compound.

2.4.4 Rheology

The rheological properties of neat PEEK and its compounds were determined on a Discovery Hybrid Rheometer DHR-1 (TA Instruments LTD®, New Castle, United States), equipped with a parallel plate geometry with a diameter of 25 mm, and a gap of less than 1 mm was applied, at 370°C. Small amplitude oscillatory shear (SAOS) experiments were performed on the samples at an angular frequency sweep from 0.1 to 100 rad/s. The linear viscoelastic response

was determined with strain amplitude sweeps from 0.05 to 12.5%, and a strain of 5% was selected for the frequency sweep tests.

2.4.5 Assessment of the compounds' thermo-mechanical stability and recycling feasibility

Neat PEEK and its compounds were submitted to consecutive reprocessing cycles with the aim to evaluate their thermo-mechanical stability and recycling feasibility. For the purpose, all compounds were subjected to 15 consecutive extrusion cycles by using the same twin-screw extruder and processing conditions described in Section 2.2. When leaving the extruder, the monofilaments were cooled in water and dried in a counter-current air dryer. Afterwards, the compounds were fed again to the extruder and the procedure was repeated 14 consecutive times. Neat and reprocessed PEEK were then characterized by Fourier Transform Infrared Spectroscopy (FTIR), using an Agilent Technologies Cary 630 spectrophotometer with an Attenuated Total Reflectance accessory (ATR) at a resolution of 4 cm^{-1} and an average of
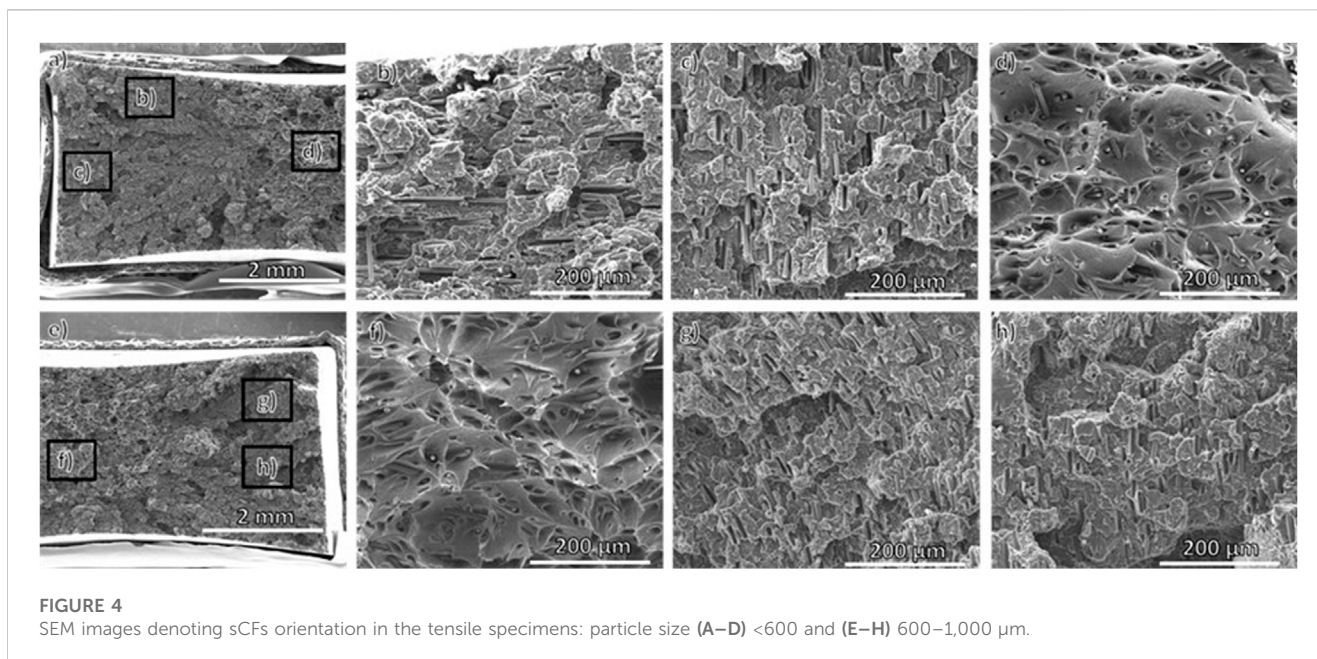
FIGURE 4
SEM images denoting sCFs orientation in the tensile specimens: particle size **(A−D)** <600 and **(E−H)** 600−1,000 μm.

140 scans. In addition, the mechanical properties of reprocessed PEEK were evaluated under conditions described previously, and the fiber length size and fiber length distribution were assessed.

2.4.6 Assessment of the compounds' fiber length and fiber length distribution after thermo-mechanical reprocessing cycles

Aiming to determine the potential fiber length reduction of the developed PEEK compounds submitted to several thermo-mechanical reprocessing cycles, the PEEK matrix of each recycled compound was removed by acid digestion, according to ASTM D3171-15. Samples with 1 g were placed in a beaker, to which 20 mL of 95%–98% sulfuric acid was carefully added. The mixture was placed on a hot plate, at 100°C for 60 min. Afterwards, 40 mL of hydrogen peroxide was added, drop by drop, to oxidize the matrix. Finally, when the solution appeared clear, CFs were washed with distilled water and acetone. After drying the fibers in an oven, at 100°C for at least 1 h, it was possible to carry out both fiber length size and fiber length distribution analysis. Optical microscopy of recovered fibers was observed by a Zeiss Axioplan 2 microscope coupled to a Zeiss AxioCam ICc 3 camera, equipped with a 6-place turret currently outfitted with 6 objectives from 5 to 100×. Scanned images of the fibers were analyzed using ImageJ software, and a scale resolution was set, in which 1 pixel corresponds to 0.8 μm.

3 Results and discussion

3.1 Particle size influence on the neat PEEK properties

The influence of two different particle sizes of rCFRT (<600 and 600–1,000 μm) on the tensile properties of neat PEEK is shown in Figure 2.

The measured tensile properties of neat PEEK, in terms of both elastic modulus and tensile strength, are similar to the values revealed by the manufacturer (4.1 GPa and 100.0 MPa vs. 3.2 ± 0.1 GPa and 98.2 ± 0.1 MPa), suggesting that a similar molecular orientation and crystallinity degree were attained in injection-molded testing samples. These observations were then confirmed by DSC data. Moreover, it can be observed that the incorporation of 5 wt% of rCFRT with larger sizes (600–1,000 μm) slightly increased the mechanical performance of neat PEEK, while a poor ability to reinforce the polymeric matrix with low load transfer efficiency seems to be attained through the incorporation of rCFRT with smaller sizes (<600 μm) (Sarasua et al., 1996), (Pan and Yapici, 2016). These results are in good agreement with studies reported in the literature (Sarasua et al., 1996; Pan and Yapici, 2016; Lu et al., 2019c).

In fact, several parameters affect the overall mechanical performance of the developed PEEK compounds, including the loading (Li et al., 2018), (Zhang et al., 2012), length (Kumar, et al, 2008), (Hirayama et al., 2017), (Unterweger et al., 2020), orientation (Subhedar et al., 2020) and dispersion level of fibers into a polymeric matrix (Nakashima et al., 2017), polymer viscosity (von Turkovich and Erwin, 2023), (Fu, et al, 2023), among others. For example, Zhang et al. (2012) showed that the strengthening mechanism of PEEK is improved by incorporating sCFs up to 10 wt%. Flexural (67.8%) and ultimate tensile strength (62.4%) enhancement were reported (Li et al., 2018) through the addition of 20 wt% of sCFs within a low-viscosity PEEK. Although higher sCFs dispersion levels are expected in polymers with a higher melt viscosity, fiber shortening can become worse due to the higher shear forces generated, limiting the reinforcement effect of sCFs (von Turkovich and Erwin, 2023), (Fu, et al, 2023). In addition, Unterweger et al. (2020) evaluated the influence of sCFs length (100–350 μm) on the mechanical properties of injection-molded composites, and the results revealed that an overall increase of both

tensile strength and elastic modulus was attained when the fiber length was increased.

After the tensile tests, the fractured surface of the specimens was observed, and the SEM images are depicted in Figure 3 A–C) for neat PEEK, D–F) < 600 μm rCFRT, and G–I) 600–1,000 μm rCFRT, respectively.

The surface of the injected-PEEK specimen evidences the presence of a smooth region, related to plastic deformation before breaking, and the appearance of necking (Figures 3A, B region A). Nevertheless, the observed necking (Chen et al., 2018) is concentrated in a region without widely spreading, while the remaining area of the specimen presents a more rough and brittle fracture surface (Figures 3A, C region B). Similar findings were observed for the PEEK compounds containing 5 wt% rCFRT, and Figures 3D, G exemplifies the regions A and B where an increased fracture roughness is visible when compared to the neat PEEK. The modified formulations showed that the sCFs are well distributed in the polymeric matrix (absence of fiber agglomerates), and sCFs pull-out and debonding are the predominant failure modes of the materials (Figures 3D, E, G, H). It is also depicted in Figures 3F, I sCFs coated with polymer sheath, which evidences the good compatibility/interaction between the fibers and the matrix. This is in agreement with the tensile results obtained, since the addition of the rCFRT did not promote a decrease of the materials' mechanical performance.

The specimens fractured surface observation also provided interesting insight on the sCFs orientation in the flow direction, from transverse section of the tensile specimens, as depicted in Figure 4.

The SEM images, in Figure 4, showed strong CFs alignment parallel to the skin region of the specimen, associated to the rapid cooling (Xiaochun et al., 2018) and the bending load applied from the vertical direction to the injection mould surface (Murata and Kanno, 2021). The core of the sample presents a more random orientation or alignment along the flow direction (Figure 4D, F). It should be noted that no difference was found between the compounds containing different sizes of sCFs (Murata and Kanno, 2021).

The influence of incorporating 5 wt% of rCFRT, with different particle sizes, on the thermal transitions and crystallization degree of neat PEEK is summarized in Figure 5 and Table 3. The onset temperature of each peak and the maximum peak temperature were identified, and the enthalpy of each transition was calculated.

The heat flow variation of neat PEEK (raw-material, in pellet form), during the first heat ramp, showed the glass transition temperature (T_g) at 165.5°C ± 0.4°C, and a single melting endotherm at 353.1°C ± 0.9°C that corresponds to the melting of the primary crystallization phase, where amorphous material nucleates and spherulitic growth occurs (higher temperature endotherm, HTE) (Pérez-Martín et al., 2022). Notice that a similar degree of crystallization was attained for the PEEK injected bars in comparison with raw-material, showing that the selected injection molding conditions were appropriate, confirming previous observations.
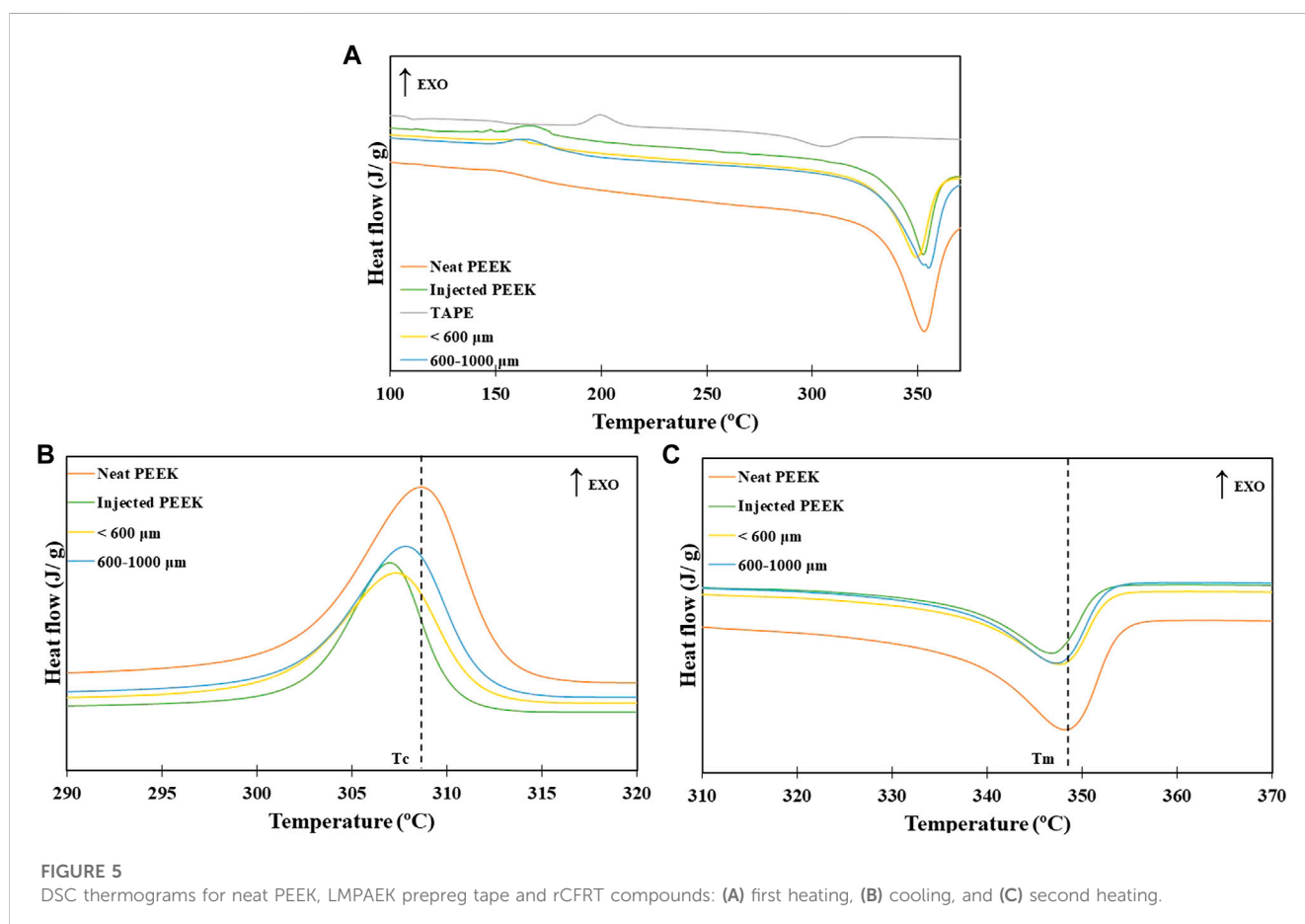

FIGURE 5
DSC thermograms for neat PEEK, LMPAEK prepreg tape and rCFRT compounds: **(A)** first heating, **(B)** cooling, and **(C)** second heating.

TABLE 3 Average values for transition temperatures and crystallinity degree of the neat PEEK and its compounds.

	T_g (°C)	ΔH_{m1} (J/g)	T_{m1} (°C)	ΔH_{m2} (J/g)	T_{m2} (°C)	X_c (%)
Neat PEEK (raw-material, pellet form)	165.5 ± 0.4	55.4 ± 3.5	353.1 ± 0.9	40.5 ± 0.5	347.0 ± 0.3	31.2 ± 0.4
PEEK (injected bars)	175.7 ± 0.2	58.2 ± 0.8	352.2 ± 0.0	40.8 ± 0.2	346.8 ± 0.0	31.2 ± 0.3
< 600 μm	169.0 ± 4.1	54.9 ± 0.2	350.4 ± 1.2	38.8 ± 1.4	347.3 ± 0.3	29.8 ± 0.9
600–1,000 μm	175.8 ± 1.4	45.3 ± 2.0	352.4 ± 1.7	36.6 ± 1.1	347.0 ± 0.0	28.2 ± 0.8

The LMPAEK prepreg tape exhibited a cold crystallization exotherm above T_g, at 199.5°C (ΔH_{cc} = 6.3 ± 0.4 J/g). This behavior is related to the processing conditions applied during prepreg tape manufacturing, where a higher cooling rate from the melt can inhibit polymer chain reorganization and crystal structure formation (Pérez-Martín et al., 2021). Therefore, the amorphous phase present in the LMPAEK prepreg tape undergoes cold crystallization during subsequent heating (Figure 5A).

The crystallization peak of compounds containing 5 wt% of rCFRT shifts to lower temperatures comparatively to PEEK (Figure 5B), indicating that the polymer recrystallization was slightly hindered in the presence of rCFRT, especially for those with larger dimensions (600–1,000 μm). However, the enthalpies associated to the first and second melting processes (Table 1) are different, suggesting that some residual stresses were generated during compounds manufacturing. In addition, it is important to note that the crystallization degree of PEEK compounds is lower than neat PEEK, which means that higher mechanical improvements through the incorporation of rCFRT could be achieved by controlling the processing conditions applied in the extrusion and injection molding.
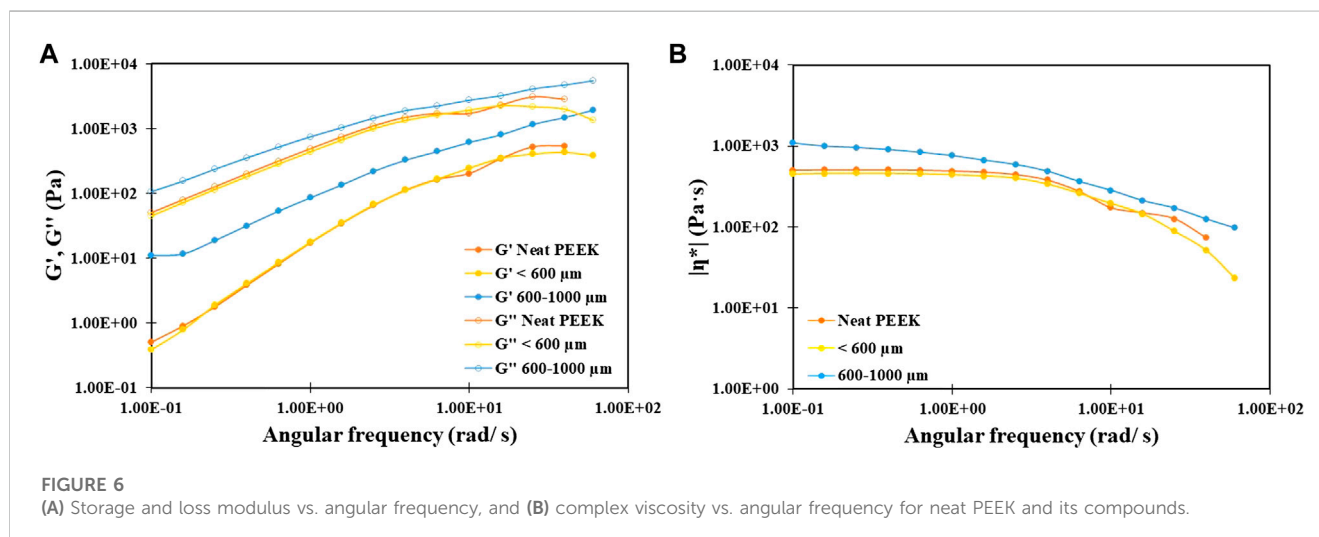
Since the incorporation of rCFRT can induce significant changes in the flow behavior of neat PEEK, and its processability limit, promoted by increments in the viscosity, the rheological properties were investigated (Rieger et al., 2019). The storage modulus (G′) is the most sensible to structural changes, and it is clo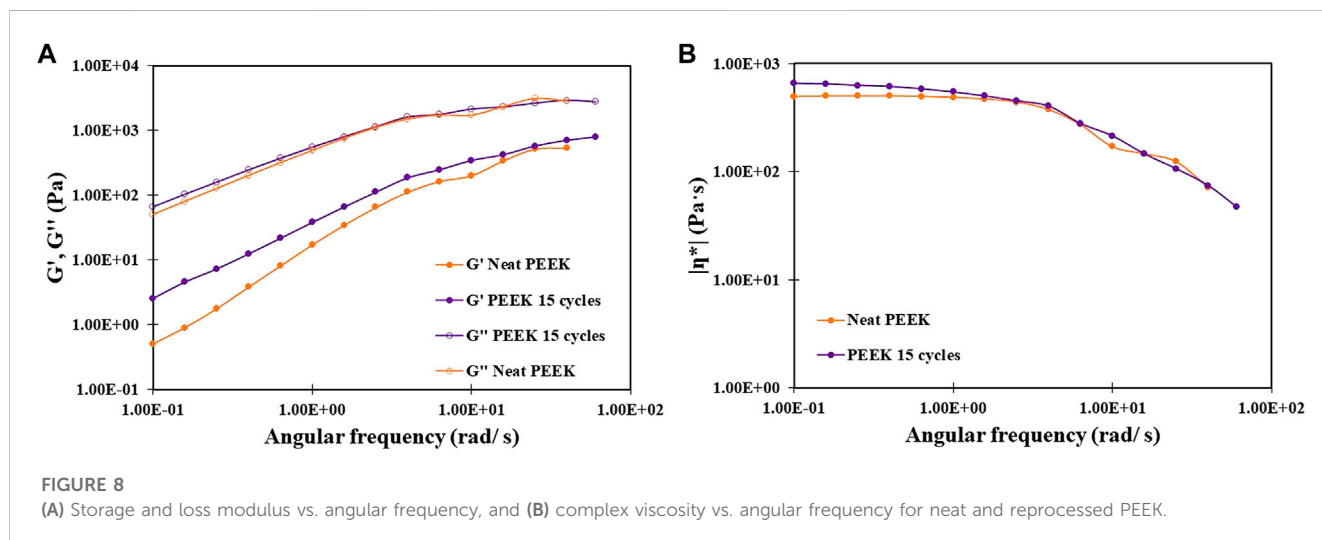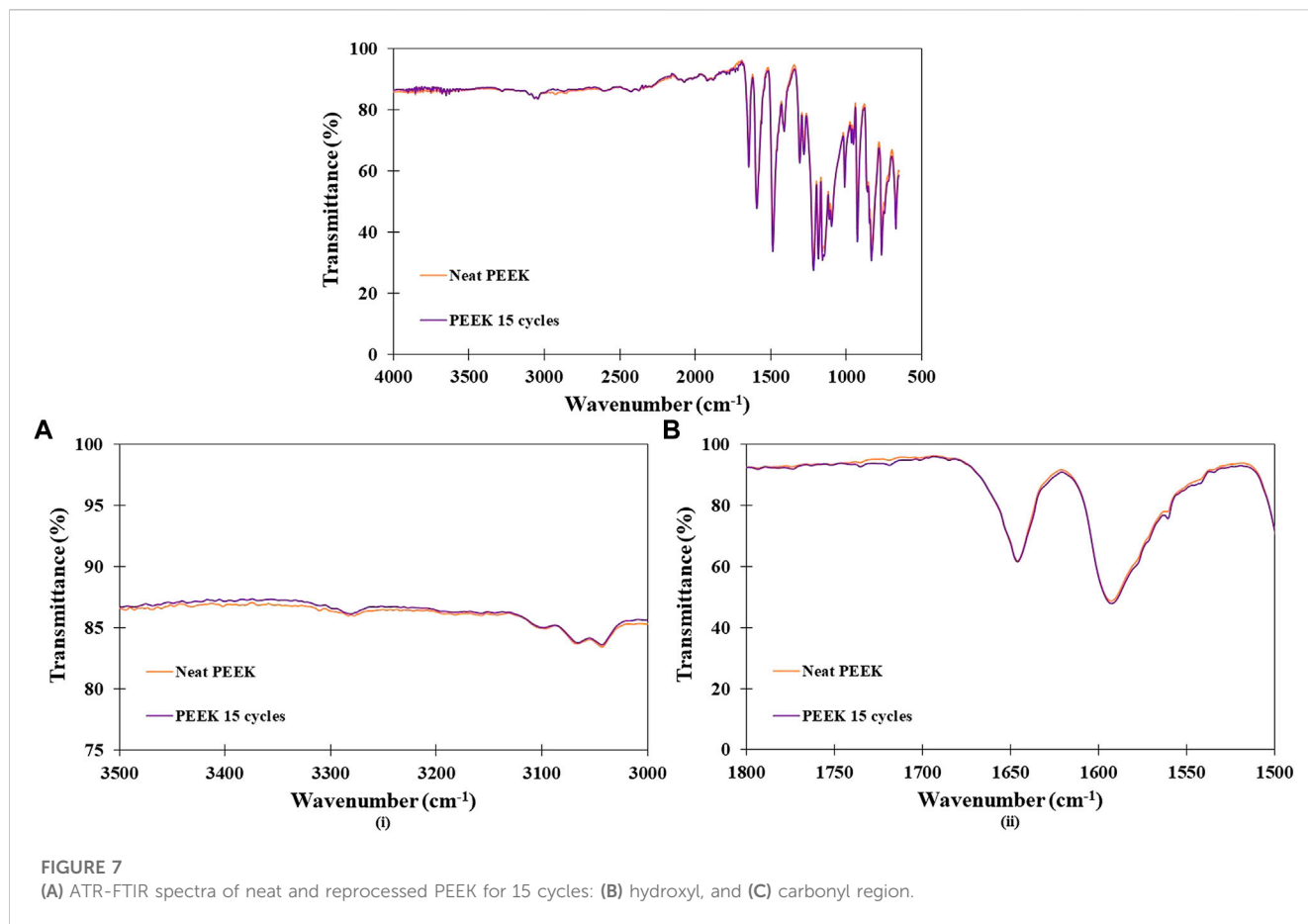sely related to the rigidity of the polymer macromolecules and their entanglement, while the loss modulus (G″) depends on the linkages that control the conformational changes of the chain segments, and the displacement of one chain in relation to another. Understanding their behavior provides essential information about the viscoelasticity of the material (Erbetta et al., 2014). Thus, the rheological characterization of neat PEEK and its compounds, including the G′, G″ and complex viscosity (|η*|) was performed, and the results are depicted in Figure 6.

For all tested formulations, G″ remained virtually unchanged since its behavior is dominated by the flow of the viscous phase, which indicates that the viscous component of the material dominates the elastic counterpart, across almost all frequencies. Higher values of G″ at the low angular frequency in comparison with neat PEEK were observed, mainly due to the presence of the solid phase (rCFRT) (Cox and Merz, 1958). Moreover, the incorporation of rCFRT slightly altered the complex viscosity of the polymeric matrix, becoming more pronounced for compounds containing larger particle sizes (600–1,000 μm).

3.2 Thermo-mechanical cycles influence on PEEK stability

The stability of neat PEEK during processing and reprocessing was evaluated, allowing to mimic its feasibility to be recycled without significant thermo-oxidative degradation and irreversible loss of properties (von Turkovich and Erwin, 2023). For this purpose, neat

FIGURE 6
(A) Storage and loss modulus vs. angular frequency, and (B) complex viscosity vs. angular frequency for neat PEEK and its compounds.

FIGURE 7
(A) ATR-FTIR spectra of neat and reprocessed PEEK for 15 cycles: **(B)** hydroxyl, and **(C)** carbonyl region.

FIGURE 8
(A) Storage and loss modulus vs. angular frequency, and **(B)** complex viscosity vs. angular frequency for neat and reprocessed PEEK.
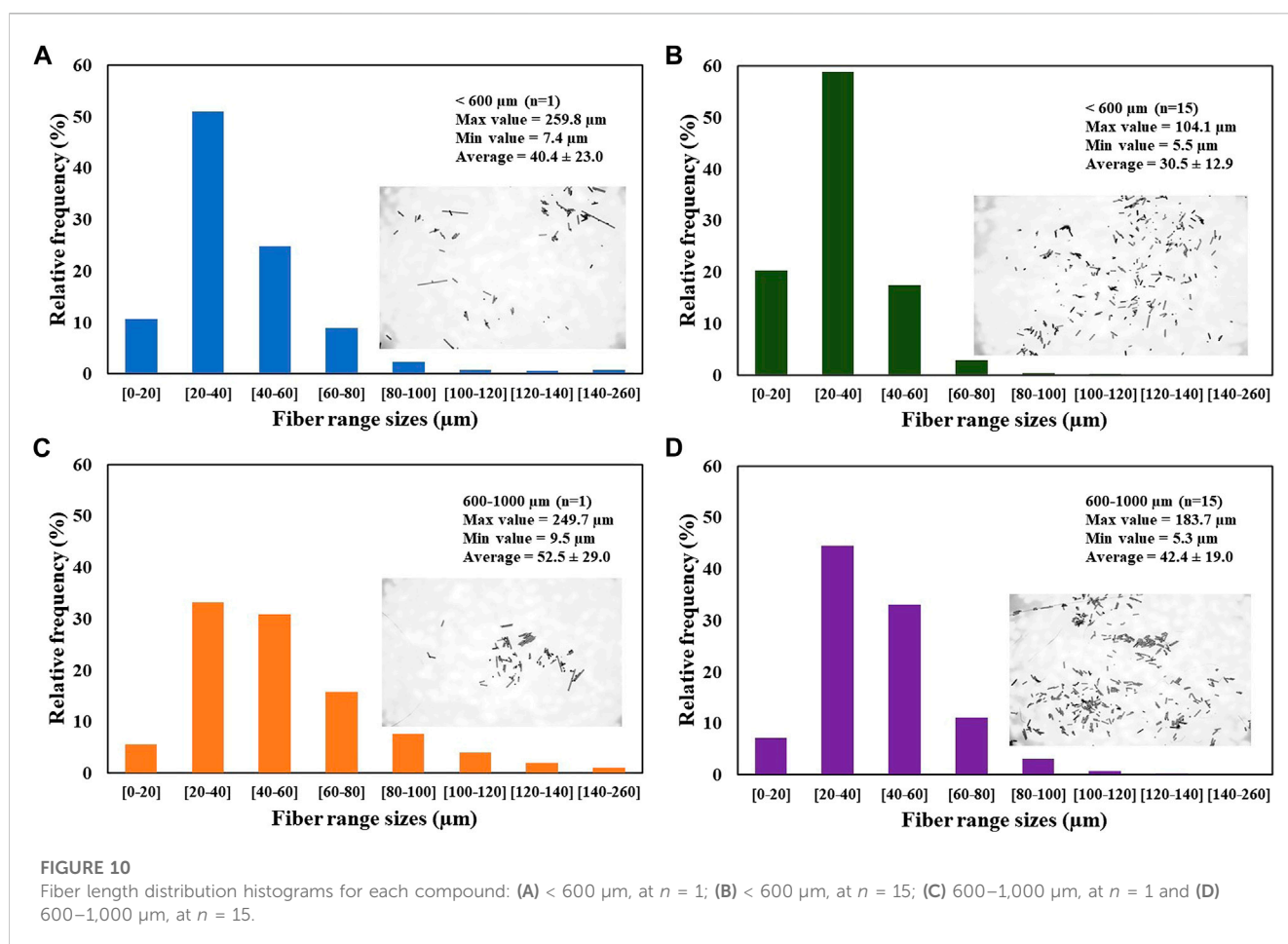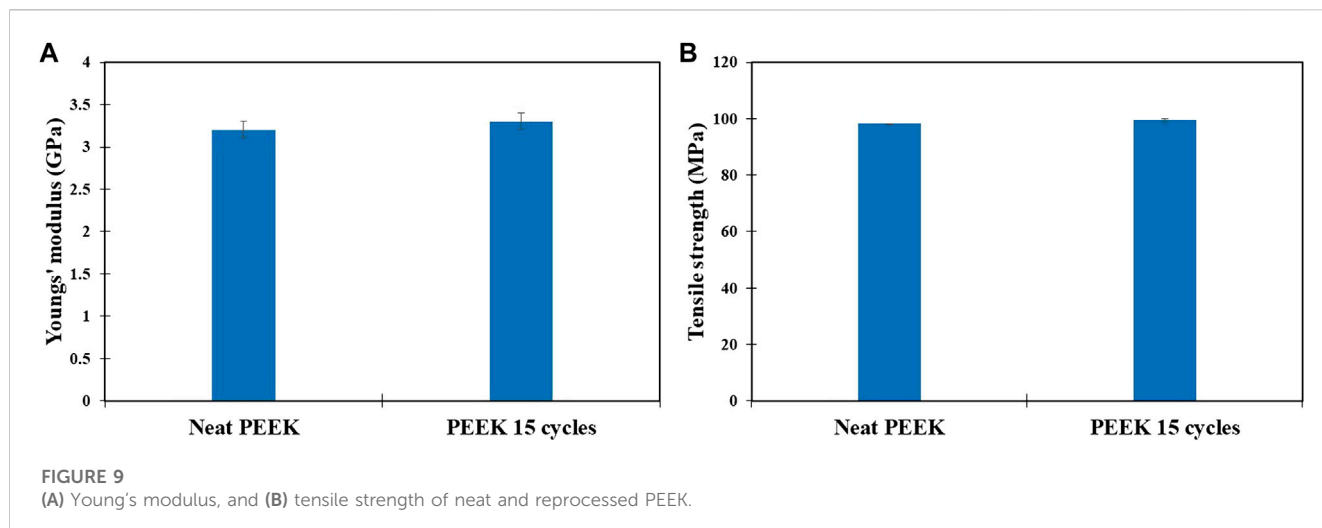
PEEK was subjected to 15 consecutive extrusion cycles under similar processing conditions. Chemical modifications that can occur on neat PEEK were followed by ATR-FTIR spectroscopy. The spectra of neat and reprocessed PEEK for 15 cycles are presented in Figure 7.

The neat PEEK showed characteristic absorption bands at 1,413, 1,490 and 1,596 cm^{-1}, attributed to stretching of the phenyl ring, while C-H deformations are mainly found in the range of

$1,200–600$ cm^{-1}. Aromatic hydrogens can be observed below 900 cm^{-1} (Gaitanelis et al., 2022). The carbonyl stretching vibration appeared at 1,646 cm^{-1}, and the bending motion of the (C-C(C=O)-C) group at 1,305 cm^{-1}. In addition, absorption bands at 1,184 and 1,219 cm^{-1} were found, and attributed to the symmetric and asymmetric stretching vibrations of the diphenyl ether group (C-O-C linkages) (Yaragalla et al., 2021).

FIGURE 9
(A) Young's modulus, and **(B)** tensile strength of neat and reprocessed PEEK.

FIGURE 10
Fiber length distribution histograms for each compound: **(A)** < 600 μm, at n = 1; **(B)** < 600 μm, at n = 15; **(C)** 600−1,000 μm, at n = 1 and **(D)** 600−1,000 μm, at n = 15.

Thermo-oxidative and/or -mechanical degradation can induce the appearance of new absorption bands or a growth of the bands intensity in the region corresponding to carbonyl (1,600–1800 cm^{-1}, Figure 8A) and hydroxyl (3,000–3,400 cm^{-1}, Figure 8B) stretching vibrations. Spectra modifications in non-aromatic hydrogen carbon bonds (2,800–3,000 cm^{-1}), can be also observed depending on the

predominant degradation mechanism, e.g., crosslinking or chain scission.

The comparison of neat and reprocessed PEEK spectra showed similar absorption bands with the same intensities, proving that no degradation was found for PEEK upon 15 extrusion cycles. Moreover, rheological measurements were performed to support

TABLE 4 Compounds' fiber-length distribution.

	Maximum value (μm)	Minimum value (μm)	Average value (μm)
< 600 μm (n = 1)	259.8	7.4	40.4 ± 23.0
< 600 μm (n = 15)	104.1	5.5	30.5 ± 12.9
600–1,000 μm (n = 1)	249.7	9.5	52.5 ± 29.0
600–1,000 μm (n = 15)	183.7	5.3	42.4 ± 19.0

previous findings observed by ATR-FTIR, and to monitor the stability of reprocessed PEEK. The rheological results are illustrated in Figure 8.

Multiple heat treatment cycles, with prolonged heating above the polymer's melting temperature, may lead to a significant change in the polymer's viscosity, which is influenced by the degradation mechanism and kinetics, or the competition between crosslinking or scission (Colin and Tcharkhtchi, 2013), (Selvanarayanan, 2017). However, the collected viscoelastic data allows to state that 15 reprocessing cycles do not promote any changes on the rheological behavior of PEEK.

Therefore, based on these results, no irreversible changes in the properties of reprocessed PEEK are expected. Aiming at confirming these considerations, the mechanical performance of reprocessed PEEK was evaluated by stress-strain experiments, and the results are shown in Figure 9.

A similar mechanical behavior was found for neat and reprocessed PEEK for consecutive 15 extrusion cycles, showing the remarkable thermal stability of PEEK even when submitted to high shear stresses, temperatures, and residence times. An important contribution to the subject was reported by A.R. et al. (McLauchlin et al., 2014) where the reprocessability of PEEK through multiple injection molding cycles was evaluated, and the results showed that the tensile strength remained almost unchanged. In addition, McLaudhlin, A. and co-workers (VICTREX, 2022) verified a similar behavior after 10 reprocessing cycles, showing the high recycling potential of this thermoplastic. Therefore, it can be concluded that the operating conditions selected for this study are suitable for the

PEEK processing and reprocessing without any signal of degradation or loss of properties.

3.3 Compounds' reprocessing influence on the material stability

The thermo-mechanical stability of PEEK compounds containing 5 wt% of rCFRT, with two different sizes, was also evaluated. The fiber length and fiber length distribution after 1 and 15 extrusion cycles were investigated, since it is well established in the literature that both extrusion and injection molding processes can induce fiber shortening, and consequently, a deterioration of the final mechanical properties of the compound (von Turkovich and Erwin, 2023), (Fu et al., 2002). There are three main causes related to this behavior: i) fiber/fiber interaction—abrasion between fiber surfaces induces stress concentrations, decreasing strength and leading to fiber fracture or bending stresses by fiber overlap, ii) fiber interaction with the polymeric matrix—viscous forces imparted by the polymer may originate fiber fracture, and iii) fiber contact with equipment surfaces occurs due to wear of the processing machine (von Turkovich and Erwin, 2023), (Fu et al., 2002).

The processing effect on fiber length was carried out for the first (n = 1) and the last (n = 15) extrusion cycle, allowing to compare the average values obtained from composite fiber length distribution among its recyclability. Figure 10 shows the fiber length distribution histograms for each compound, at n = 1 and n = 15.
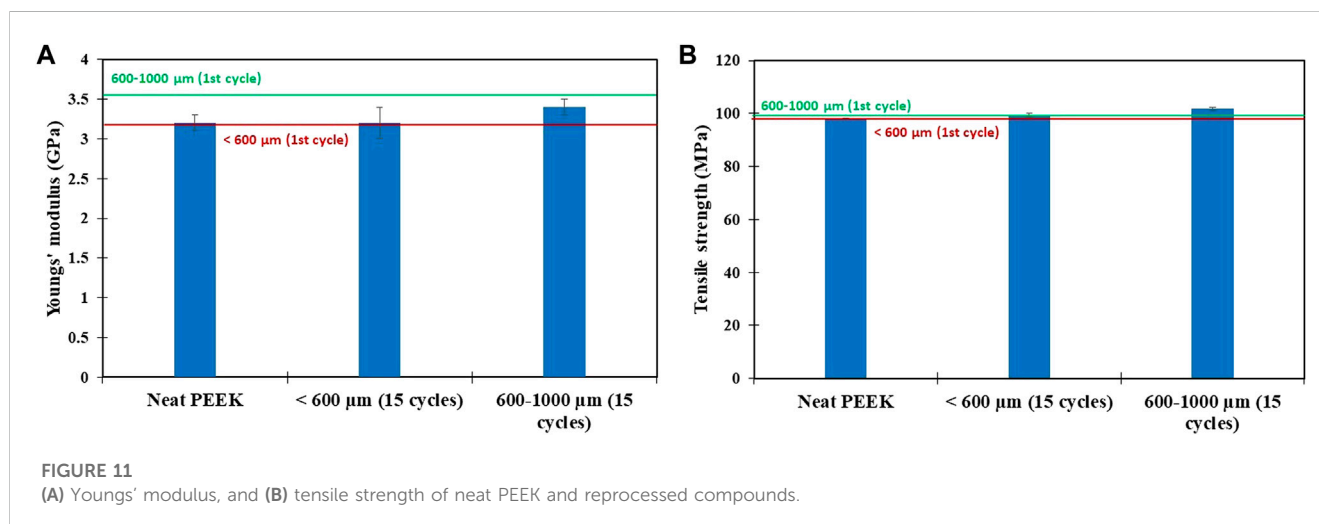

FIGURE 11
(A) Youngs' modulus, and (B) tensile strength of neat PEEK and reprocessed compounds.

The results of the analysis of the obtained fiber length distribution of the compounds are represented in Table 4.

For both formulations, a significant decrease in fiber length was observed right after the first reprocessing cycle, although sCFs shortening is more pronounced for larger particle sizes. In addition, promoted by fiber breakage, the number of smaller fibers increased. After 15 extrusion cycles, this trend is maintained although the average fiber length decreases by being much lower.

Since the reinforcement of PEEK is related to the fiber length of rCFRT, the mechanical characterization of reprocessed compounds for 15 cycles was also assessed by uniaxial tensile tests, and the results are depicted in Figure 11.

It can be observed that reprocessed PEEK compounds containing 5 wt% of rCFRT, with different particle sizes, exhibited similar tensile strength behavior when compared to the PEEK compounds submitted to a single extrusion cycle. However, the formulation containing larger sCF particles demonstrated a slight decrease on the Youngs' modulus, in comparison to the same formulation submitted to a single extrusion cycle. Previous findings attained by optical microscopy support this behavior, once the pronounced reduction of fiber length occurred right after the first extrusion cycle, being more significant for larger sCF.

4 Conclusion

In this work, "waste" scraps from CFRP were incorporated into a thermoplastic matrix (PEEK), for a second-life in the aeronautic industry. The effect of two different fiber particle sizes (<600 μm and 600–1,000 μm rCFRT) on the mechanical, thermal and rheological properties of produced PEEK compounds, was assessed. The mechanical properties of the compounds did not increase significantly, which could be a result not only from the fiber breakage during material processing or the low content of rCFRT incorporation, but also from the lower degree of crystallization obtained. Nevertheless, the sCF were well distributed into the polymeric matrix and presented good fiber/matrix interface. In terms of the rheological characterization, it is concluded that the highest values of the storage modulus in the low angular frequency region are due to the presence of the solid phase, the viscous component of the material dominates the elastic counterpart across all frequencies, and the material viscosity slight increases in the presence of rCFRT.

Empowering an eco-friendly strategy, reprocessing studies were performed to evaluate the thermoplastic matrix and compounds' recyclability. For this purpose, the material was submitted to 15 consecutive extrusion cycles, for further characterization. Results obtained by ATR-FTIR showed that similar absorption bands with comparable intensities were obtained for both neat and reprocessed PEEK, proving that no degradation occurred nor loss of properties. These findings were supported by viscoelastic and mechanical data. Therefore, it can be concluded that the selected processing and reprocessing conditions for the developing materials were appropriate. The fiber length and fiber length distribution upon 15 extrusion cycles were assessed and the mechanical behavior was also evaluated. It can be concluded that both formulations with different particle sizes exhibited similar tensile strength behavior, while the compound containing larger sCF showed a decrease of the Young's Modulus when compared to the same formulations submitted to a single extruder cycle. The results on the fiber length support this behavior once the pronounced reduction of fiber length occurred right after the first extrusion cycle, being more significant for larger sCF.

Data availability statement

The raw data supporting the conclusion of this article will be made available by the authors, without undue reservation.

Author contributions

Contributions on experimental work developed, including compounding and characterization: CB and AA; original draft: CB and AC; acquisition of the financial support for the project leading to this publication: RS and JS; conceptualization, formal analysis, and supervision: RS; review and editing: All. All authors contributed to the article and approved the submitted version.

Funding

Conflict of interest

The authors declare that the research was conducted in the absence of any commercial or financial relationships that could be construed as a potential conflict of interest.

Publisher's note

All claims expressed in this article are solely those of the authors and do not necessarily represent those of their affiliated organizations, or those of the publisher, the editors and the reviewers. Any product that may be evaluated in this article, or claim that may be made by its manufacturer, is not guaranteed or endorsed by the publisher.

References

Al-Lami, A., Hilmer, P., and Sinapius, M. (2018). Eco-efficiency assessment of manufacturing carbon fiber reinforced polymers (CFRP) in aerospace industry. *Aerosp. Sci. Technol.* 79, 669–678. doi:10.1016/j.ast.2018.06.020

Alshammari, B. A., Alsuhybani, M. S., Almushaikeh, A. M., Alotaibi, B. M., Alenad, A. M., Alqahtani, N. B., et al. (2021). Comprehensive review of the properties and modifications of carbon fiber-reinforced thermoplastic composites. *Polymers* 13 (15), 2474. doi:10.3390/polym13152474

Alves, S. M. C., da Silva, F. S., Donadon, M. V., Garcia, R. R., and Corat, E. J. (2018). Process and characterization of reclaimed carbon fiber composites by pyrolysis and oxidation, assisted by thermal plasma to avoid pollutants emissions. *J. Compos. Mater.* 52 (10), 1379–1398. doi:10.1177/0021998317724214

Butenegro, J. A., Bahrami, M., Abenojar, J., and Martínez, M. Á. (2021). Recent progress in carbon fiber reinforced polymers recycling: A review of recycling methods and reuse of carbon fibers. *Materials* 14, 6401–6421. doi:10.3390/ma14216401

Carberry, W. *Airplane recycling efforts benefit boeing operators*. Seattle, Washington D.C, United States:2006 Boeing AERO Magazine.

Chen, C., Zhang, C., Liu, C., Miao, Y., Wong, S. C., and Li, Y. (2018). Rate-dependent tensile failure behavior of short fiber reinforced PEEK. *Compos B Eng.* 136, 187–196. doi:10.1016/j.compositesb.2017.10.031

Colin, X., and Tcharkhtchi, A. (2013). Thermal degradation of polymers during their mechanical recycling. Recycling: Technological systems, management practices and environmental impact. *Nova Sci.*, 57–95.

Cox, W. P., and Merz, E. H. (1958). Correlation of dynamic and steady flow viscosities. *J. Polym. Sci.* 28, 619–622. doi:10.1002/pol.1958.1202811812

Elsayed, A., and Roetger, T. (2022). *Best practices and standards in aircraft end-of-life and recycling*. Montreal, Canada: ICAO.

Erbetta, C. D. C., Manoel, G. F., Oliveira, A. P. L. R., e Silva, M. E. S. R., Freitas, R. F. S., and Sousa, R. G. (2014). Rheological and thermal behavior of high-density polyethylene (HDPE) at different temperatures. *Mater. Sci. Appl.* 5 (13), 923–931. doi:10.4236/msa.2014.513094

Fortune Business Insights (2023). *Carbon Fiber Market Size, Share & COVID-19 Impact Analysis, By Precursor (PAN and Pitch), By Tow (Large Tow and Small Tow), By Application (Aviation, Aerospace & Defense, Automotive, Wind Turbines, Sports & Leisure, Construction, and Others), and Regional Forecast, 2023–2030*.

Fu, S.-Y., Mai, Y.-W., Chui, E., Ching, Y., and Li, R. K. Y. (2002). Correction of the measurement of fiber length of short fiber reinforced thermoplastics. *Compos. Part A Appl. Sci. Manuf.* 33, 1549–1555. doi:10.1016/S1359-835X(02)00114-8

Fu, S.-Y., Mai, Y.-W., Chui, E., Ching, Y., and Li, R. K. Y. Correction of the measurement of fiber length of short fiber reinforced thermoplastics.2023 Available: www.elsevier.com/locate/compositesa.

Gaitanelis, D., Worrall, C., and Kazilas, M. (2022). Detecting, characterising and assessing PEEK's and CF-PEEK's thermal degradation in rapid high-temperature processing. *Polym. Degrad. Stab.* 204, 110096. doi:10.1016/j.polymdegradstab.2022.110096

Gao, S., Qu, J., Li, H., and Kang, R. (2022). Effect of fiber type and content on mechanical property and lapping machinability of fiber-reinforced polyetheretherketone. *Polym. (Basel)* 14 (6), 1079. doi:10.3390/polym14061079

Giorgini, L., Benelli, T., Brancolini, G., and Mazzocchetti, L. (2020). Recycling of carbon fiber reinforced composite waste to close their life cycle in a cradle-to-cradle approach. *Curr. Opin. Green Sustain. Chem.* 26, 100368. doi:10.1016/j.cogsc.2020.100368

Hirayama, D., Saron, C., Botelho, E. C., Costa, M. L., and Junior, A. C. A. (2017). "Polypropylene composites manufactured from recycled carbon fibers from aeronautic materials waste," in *Materials research* (São Carlos, Brazil: Universidade Federal de Sao Carlos), 526–531. doi:10.1590/1980-5373-MR-2016-1022

IATA (2022). *Helping aircraft decommissioning*. Montreal, Canada: IATA.

Kumar, K. S. S., Nair, C. P. R., and Ninan, K. N. (2008). Effect of fiber length and composition on mechanical properties of carbon fiber-reinforced polybenzoxazine. *Polym. Adv. Technol.* 19 (7), 895–904. doi:10.1002/pat.1056

Li, F., Hu, Y., Hou, X., Hu, X., and Jiang, D. (2018). Thermal, mechanical, and tribological properties of short carbon fibers/PEEK composites. *High. Perform. Polym.* 30 (6), 657–666. doi:10.1177/0954008317715313

Li, H., and Englund, K. (2017). Recycling of carbon fiber-reinforced thermoplastic composite wastes from the aerospace industry. *J. Compos Mater* 51 (9), 1265–1273. doi:10.1177/0021998316671796

Liu, T., Shao, L., Zhao, B., Chang, Y. C., and Zhang, J. (2022). Progress in chemical recycling of carbon fiber reinforced epoxy composites. *Macromol. Rapid Commun.* 43 (23), 2200538. doi:10.1002/marc.202200538

Lu, C., Ma, W., Ba, S., and Zhang, D. (2023). Resin content calculation of carbon fiber/poly (ether ether ketone) by thermogravimetric analysis. *Polym. Test.* 117, 107861. doi:10.1016/j.polymertesting.2022.107861

Lu, C., Xu, N., Zheng, T., Zhang, X., Lv, H., Lu, X., et al. (2019a). The optimization of process parameters and characterization of high-performance CF/PEEK composites prepared by flexible CF/PEEK plain weave fabrics. *Polym. (Basel)* 11 (1), 53. doi:10.3390/polym11010053

Lu, C., Xu, N., Zheng, T., Zhang, X., Lv, H., Lu, X., et al. (2019b). The optimization of process parameters and characterization of high-performance CF/PEEK composites prepared by flexible CF/PEEK plain weave fabrics. *Polym. (Basel)* 11 (1), 53. doi:10.3390/polym11010053

Lu, C., Xu, N., Zheng, T., Zhang, X., Lv, H., Lu, X., et al. (2019c). The optimization of process parameters and characterization of high-performance CF/PEEK composites prepared by flexible CF/PEEK plain weave fabrics. *Polym. (Basel)* 11 (1), 53. doi:10.3390/polym11010053

McLauchlin, A. R., Ghita, O. R., and Savage, L. (2014). Studies on the reprocessability of poly(ether ether ketone) (PEEK). *J. Mater Process Technol.* 214 (1), 75–80. doi:10.1016/j.jmatprotec.2013.07.010

Meng, F., Cui, Y., Pickering, S., and McKechnie, J. (2020). From aviation to aviation: Environmental and financial viability of closed-loop recycling of carbon fibre composite. *Compos B Eng.* 200, 108362. doi:10.1016/j.compositesb.2020.108362

Murata, Y., and Kanno, R. (2021). Effects of heating and cooling of injection mold cavity surface and melt flow control on properties of carbon fiber reinforced semi-aromatic polyamide molded products. *Polymers* 13, 587. doi:10.3390/polym13040587

Nakashima, Y., Suganuma, H., Yamashita, S., and Takahashi, J. "Influence of strand dispersion method on mechanical properties of randomly oriented carbon fiber strand thermoplastic composites," in Proceedings of the 21st International Conference on Composite Materials, Xi'an, China, August 2017.

Nikhil, M., Bilagi, C., and Eswara, P. (2022). Carbon fiber reinforced plastic (CFRP) market by raw material (polyacrylonitrile (PAN), petroleum pitch, and others), resin type (thermosetting and thermoplastic), and application (aerospace & defense, wind turbine, automotive, sports equipment, building & construction, and others). *Glob. Oppor. Analysis Industry Forecast*.

Oliveux, G., Dandy, L. O., and Leeke, G. A. (2015). Current status of recycling of fibre reinforced polymers: Review of technologies, reuse and resulting properties. *Prog. Mater. Sci.* 72, 61–99. doi:10.1016/j.pmatsci.2015.01.004

Pan, L., and Yapici, U. (2016). A comparative study on mechanical properties of carbon fiber/PEEK composites. *Adv. Compos. Mater.* 25 (4), 359–374. doi:10.1080/09243046.2014.996961

Pedoto, G., Grandidier, J. C., Gigliotti, M., and Vinet, A. (2022). Characterization and modelling of the PEKK thermomechanical and creep behavior above the glass transition temperature. *Mech. Mater.* 166, 104189. doi:10.1016/j.mechmat.2021.104189

Pérez-Martín, H., Mackenzie, P., Baidak, A., Ó Brádaigh, C. M., and Ray, D. (2021). Crystallinity studies of pekk and carbon fibre/PEKK composites: A review. *Compos. Part B Eng.* 223, 109127. doi:10.1016/j.compositesb.2021.109127

Pérez-Martín, H., Mackenzie, P., Baidak, A., Ó Brádaigh, C. M., and Ray, D. (2022). Crystallisation behaviour and morphological studies of PEKK and carbon fibre/PEKK composites. *Compos Part A Appl. Sci. Manuf.* 159, 1–18. doi:10.1016/j.compositesa.2022.106992

Petrauskaite, G. (2022). The afterlife of retired aircraft: What are old planes turned into? *Aerotime Hub*.

Pimenta, S., and Pinho, S. T. (2011). Recycling carbon fibre reinforced polymers for structural applications: Technology review and market outlook. *Waste Manag.* 31 (2), 378–392. doi:10.1016/j.wasman.2010.09.019

Pulkkinen, A. (2022). The global composites market is driven by Carbon Fiber Reinforced Plastics. https://nordicgrowth.com/en/the-global-composites-market-is-driven-by-carbon-fiber-reinforced-plastics/.

Rieger, D., Pola, M., Franče, P., Kadlec, J., Kovářík, T., and Kopačka, P. (2019). The effect of short carbon fibers on rheological behaviour and mechanical properties of metakaolin-slag geopolymer binder. *IOP Conf. Ser. Mater. Sci. Eng.* 613, 012050. doi:10.1088/1757-899X/613/1/012050

Sarasua, J. R., Remiro, P. M., and Pouyet, J. (1996). Effects of thermal history on mechanical behavior of PEEK and its short-fiber composites. *Polym. Compos* 17 (3), 468–477. doi:10.1002/pc.10635

Selvanarayanan, H. (2017). *Effects of thermal degradation on carbon reinforced PEEK composites*. Delft, Netherlands: TU Delft.

Subhedar, K., (2020). Effect of fibre orientation on mechanical properties of carbon fibre composites SEE PROFILE Effect of fibre orientation on mechanical properties of carbon fibre composites. Available: https://www.researchgate.net/publication/350809879.

Sudhin, S. A., Remanan, M., and Jayanarayanan, K. (2020). Comparison of properties of carbon fiber reinforced thermoplastic and thermosetting composites for aerospace applications. Available:www.sciencedirect.com.

Unterweger, C., Mayrhofer, T., Piana, F., Duchoslav, J., Stifter, D., Poitzsch, C., et al. (2020). Impact of fiber length and fiber content on the mechanical properties and electrical conductivity of short carbon fiber reinforced polypropylene composites. *Compos Sci. Technol.* 188, 107998. doi:10.1016/j.compscitech.2020.107998

Victrex (2022). The use of regrind with VICTREX® PEEK. https://www.victrex.com/.

Vincent, G. A., de Bruijn, T. A., Wijskamp, S., Abdul Rasheed, M. I., van Drongelen, M., and Akkerman, R. (2019). Shredding and sieving thermoplastic composite scrap: Method development and analyses of the fibre length distributions. *Compos B Eng.* 176, 107197. doi:10.1016/j.compositesb.2019.107197

Vo Dong, P. A., Azzaro-Pantel, C., and Cadene, A. L. (2018). Economic and environmental assessment of recovery and disposal pathways for CFRP waste management. *Resour. Conserv. Recycl* 133, 63–75. doi:10.1016/j.resconrec.2018.01.024

von Turkovich, R., and Erwin, L. (2023). Fiber fracture in reinforced thermoplastic processing. *Polym. Eng. Sci.* 63.

Xiaochun, Y., Youhua, Y., Yanhong, F., Guizhen, Z., and Jinsong, W. (2018). Preparation and characterization of carbon fiber/polypropylene composites via a tri-screw in-line compounding and injection molding. *Adv. Polym. Technol.* 37 (8), 3861–3872. doi:10.1002/adv.22169

Yao, S. S., Jin, F. L., Rhee, K. Y., Hui, D., and Park, S. J. (2018). Recent advances in carbon-fiber-reinforced thermoplastic composites: A review. *Compos. Part B Eng.* 142, 241–250. doi:10.1016/j.compositesb.2017.12.007

Yaragalla, S., Zahid, M., Panda, J. K., Tsagarakis, N., Cingolani, R., and Athanassiou, A. (2021). Comprehensive enhancement in thermomechanical performance of melt-extruded peek filaments by graphene incorporation. *Polym. (Basel)* 13 (9), 1425. doi:10.3390/polym13091425

Zhang, J., Chevali, V. S., Wang, H., and Wang, C. H. (2020a). Current status of carbon fibre and carbon fibre composites recycling. *Compos. Part B Eng.* 193, 108053. doi:10.1016/j.compositesb.2020.108053

Zhang, J., Chevali, V. S., Wang, H., and Wang, C. H. (2020b). Current status of carbon fibre and carbon fibre composites recycling. *Compos. Part B Eng.* 193, 108053. doi:10.1016/j.compositesb.2020.108053

Zhang, L., Li, M., and Hu, H. (2012). "Study on mechanical properties of PEEK composites," in *Advanced materials research* (Wollerau, Switzerland: Trans Tech Publications Ltd), 519–525. doi:10.4028/www.scientific.net/AMR.476-478.519